Vector field guidance for path following of MAVs in three dimensions for variable altitude maneuvers

Vaitheeswaran S.Meenakshisundaram, Venkatanarayana K. Gundappa
Aerospace Electronics and Systems Division, National Aerospace Laboratories, Council of Scientific and Industrial Research, Bangalore, INDIA 560017

B. Sashi Kanth
Indian Institute of Technology, Madras, Chennai, INDIA

Received on 22nd July 2010; Accepted on 3rd December 2010

ABSTRACT

This paper uses the vector field approach to represent both the desired ground track heading and the vertical flight path angle to navigate unmanned aerial vehicles onto the desired path. The path following is realized in 3-dimensions, thus allowing the aircraft to navigate longitudinally as well as laterally, unlike the current approaches which require the aircraft to maintain a constant altitude. This results in an increase in the maneuverability (like overflying a hill) of the vehicle allowing it to navigate over various terrains and terrain following. Methods for following straight lines in 3-dimensional space are demonstrated through numerical simulations.

1. INTRODUCTION

Over the past several years Miniature Aerial Vehicles (MAVs) have received considerable attention for many useful applications ranging from battlefield surveillance , smart munitions and real time bomb damage assessment to forest –fire reconnaissance, surveys of natural disaster areas and inexpensive traffic and accident monitoring [1-10]. In this, the ability of the MAV to fly in constrained environments is an important requirement for both civil and military applications. Whether in corridors defined by streets/high rise buildings or over different terrains MAVs are required to fly amidst both natural and man-made obstacles. Unlike piloted vehicles, which rely on the pilot to navigate over demanding terrain or to avoid obstructions, MAVs rely on pre planning and automation to provide this functionality. Given a terrain map, safe flight paths are generated using a set of waypoints and the capability to plan paths and follow them precisely is of great importance in MAV applications. For a set of ordered waypoints specifying a desired flight path, a higher level algorithm is used to generate desired flight trajectories to drive the vehicle to its path.

With the path specified by a sequence of ordered waypoints, there are two general approaches to the path planning problem. In the first approach, the vehicle is made to follow a reference point, which travels along the path at a set velocity and is referred to as trajectory tracking[11].This implicitly requires that the vehicle be in a certain position at a certain time, which can cause problems for small MAV's, where wind speeds can approach 50 or 60 percent of the aircraft's airspeed.. The second approach is a path following approach [12]. The objective in path following is that the vehicle be on the path, rather than in a certain place at a certain time. The path following algorithms use either a vector field approach or a potential field approach (PFA) [13,14] to generate the trajectory fields for the guidance problems. PFA consider obstacles as charges with repelling force and the goal position as having a charge with an attractive force. Trajectories are then calculated on the basis of the charge field. These methods have weaknesses; the most renowned is the local minima problem for the collision avoidance issue [15, 16]. The specific realization of the *Vector Field* approach [17], can be thought of as a method where 'vectors vary from point to point', and are potential fields.

In the existing approaches, Vector fields are based on a vector field construction that represents the desired ground track of the aircraft. Given the current position and the waypoint path, the vector field is essentially painted on the ground around the path. This field specifies the desired ground track headings as a function of vehicle position, groundspeed, and ground track. By directly specifying a desired ground-track (rather than a heading), the algorithms in this subsystem guarantee path convergence in the presence of constant wind disturbances, provided that the aircraft can maintain a positive groundspeed.

Most of the works reported hitherto, also simplify the navigation problem assuming a constant groundspeed as well as a constant altitude and the vector fields are essentially painted in two dimensions with the heading commands confined to a horizontal plane. It is of interest to note that some missions may require the MAV to go into a valley or over the hill and it is desirable that the heading commands be expressed also in terms of the vertical flight path angles.

The work presented in this paper builds on the concept of path following through the construction of a three dimensional vector field around the path to be followed. Controlling heading rate and the pitch rate using ground track heading and vertical flight path angle automatically accounts for the wind condition thus reducing the deleterious effect of wind. By extending the algorithm to three dimensions we allow the aircraft to vary its altitude as well. As a result, the maneuverability of the aircraft is increased allowing it to navigate in different terrains.

2. NAVIGATION EQUATIONS FOR PATH GENERATION

To achieve path following in the presence of wind, the proposed method constructs a vector field around the path to be tracked. These vectors serve as direction vectors for the MAV. The vectors define the heading and the vertical flight path angle, for the MAV to reach the desired path. The method is currently applicable to straight line paths. Figure 1(a) and 1(b) show the vector field, for linear paths, inside the transition region and outside the transition region respectively.

The vector fields are visualized as a body of water with the water flowing towards a desired line. A piece of paper which is placed in the water follows the direction of the flow of water and eventually ends up near the line to which the water flow is directed. Similarly by constructing a vector field around the path to be followed we are directing the MAV towards the path.

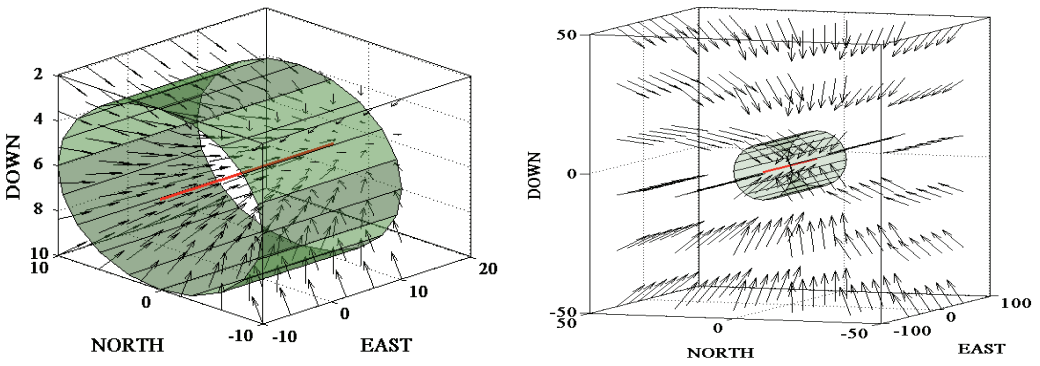

Figure 1. Vector field (a) Inside the transition region. (b) Outside the transition region. The cylinder indicates the boundary of the transition region.

The navigational dynamics in three dimensions can be described by the following set of equations:

$$\dot{x} = V \cos\psi \cos\theta + W_x \tag{1}$$

$$\dot{y} = V \sin\psi \cos\theta + W_y \tag{2}$$

$$\dot{z} = V \sin\theta \tag{3}$$

W_x and W_y are the x and y components of the wind velocity, ψ is the heading and θ the pitch angle.

An alternate approach building on the ground track heading angle (χ) and vertical flight path angle (γ) (depicted in figure 2) is developed by noting the relationship between the ground speed (S), airspeed (V) and wind speed (W).

$$\dot{x} = V_x + W_x = S_x \tag{4}$$

$$\dot{y} = V_y + W_y = S_y \tag{5}$$

$$\dot{z} = V_z = S_z \tag{6}$$

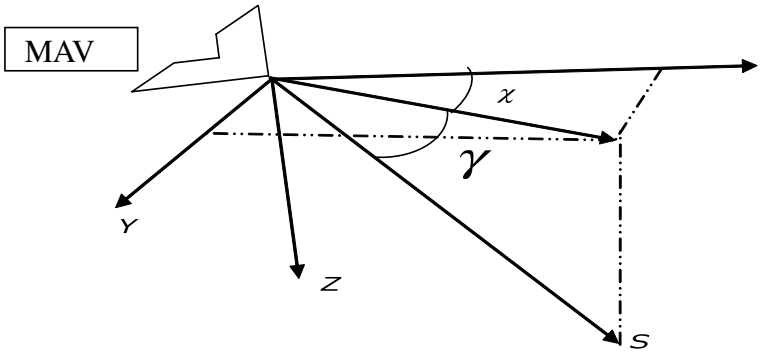

Figure 2. Illustration of the ground track heading angle and the vertical flight pathe angle.

To express the equations of motion to be independent of wind velocities, equations, (1), (2) and (3) are written as:

$$\dot{x} = S\cos\chi\cos\gamma \tag{7}$$

$$\dot{y} = S\sin\chi\cos\gamma \tag{8}$$

$$\dot{z} = S\sin\gamma \tag{9}$$

Where χ is the ground track heading angle and γ is the vertical flight path angle as shown in Figure(2). The variables in the equations χ and γ, are independent of the wind velocities and therefore when the ground based measurements are used along with the vector field approach the errors due to wind disturbances can be reduced. We will assume that the MAV is equipped with an autopilot capable of controlling the ground track heading angle χ and the vertical flight path angle γ. We want the ground track heading angle and the vertical flight path angle to tend to the commanded ground track heading χ_c and the commanded vertical flight angle γ_c which result in the following dynamics for χ and γ.

System must be in equilibrium at $\chi = \chi_c$. Therefore the first derivative must be equal to zero.

$$\Rightarrow \dot{\chi} = 0 \text{ at } \chi = \chi_c \tag{10}$$

$$\Rightarrow \dot{\chi} = \alpha(\chi_c - \chi) \tag{11}$$

α is a proportionality constant. To be in a stable equilibrium the second derivative must be less than zero.

$$\Rightarrow \ddot{\chi} \text{ at } \chi = \chi_c \tag{12}$$

$$\Rightarrow \alpha > 0 \tag{13}$$

Similarly system must be in equilibrium at $\gamma = \gamma_c$. Therefore the first derivative must be equal to zero.

$$\Rightarrow \dot{\gamma} = 0 \tag{14}$$

$$\Rightarrow \dot{\gamma} = \beta(\gamma_c - \gamma) \tag{15}$$

To be in a stable equilibrium at $\gamma = \gamma_c$. the second derivative must be less than zero.

$$\Rightarrow \ddot{\gamma} < 0 \tag{16}$$

$$\Rightarrow \beta > 0 \tag{17}$$

3. VECTOR FIELDS AND PATH FOLLOWING IN THREE DIMENSIONS

Consider the straight line indicated in Figure 1 by the solid line segment. In order for the MAV to follow this path, a vector field is constructed in the space around the straight line. When the MAV is far away from the line (distance greater than two or three times the max(minradius(χ),minradius(γ)), the objective is to fly towards the path. As the MAV approaches the path, the desired ground track heading and vertical flight path angles transition from approaching the path to flying along the path.

The transition region is visualized as a cylinder around the straight line with a radius τ. Outside the transition region the desired ground track heading and the desired vertical flight path angle are constant, and respectively equal to χ_d and γ_d. Inside the transition region χ and γ start to transition from χ_d and γ_d to χ_f and γ_f. χ_f and γ_f are ground track heading and vertical flight path angle along the desired path. Table1 displays all the variables used in the algorithm for straight line path following in 3 dimensions.

The vector fields are initially developed in cylindrical coordinates with the axis of the cylinder along the current path as this simplifies the calculations involved. The origin of this cylindrical coordinate system is assumed to be situated at the first waypoint. We next, transform the position vector of the MAV with respect to the first waypoint from the world coordinate frame into the reference frame with X-axis pointing along the path (X', Y', Z'). The vector fields in the cylindrical coordinate system are given by

$$\vec{V} = |V| \times (-\sin(\lambda_e)\hat{e}_\rho + \cos(\lambda_e)\hat{e}_z \qquad r > \tau \tag{18}$$

$$\vec{V} = |V| \times \left(-\sin\left(\frac{\lambda_e \times r}{\tau}\right)\hat{e}_p + \cos\left(\frac{\lambda_e \times r}{\tau}\right)\hat{e}_z \right) \qquad 0 < r < \tau \tag{19}$$

$$\vec{V} = |V|\hat{e}_z \qquad r = 0 \tag{20}$$

with notations given in Table I.

Since the world frame is described in Cartesian co-ordinates, the above equations are converted into Cartesian coordinate system. Let X', Y', Z' be the coordinate system where the X-axis is along the path (Path coordinate system). Note that the coordinate system has its X-axis along the path while the cylindrical coordinate system has its Z-axis along the path (Figure 3b). The vector field in the Cartesian coordinate system is given by

$$\vec{V}_{X'Y'Z'} = |V| \times (\cos(\lambda_e)\hat{e}_{x'} - \sin(\lambda_e)\cos(\varphi)\hat{e}_{y'} - \sin(\lambda_e)\sin(\varphi)\hat{e}_{z'}) \qquad r > \tau \tag{21}$$

$$\vec{V}_{X'Y'Z'} = |V| \times \left(\cos\left(\frac{\lambda_e \times r}{\tau}\right)\hat{e}_{x'} - \sin\left(\frac{\lambda_e \times r}{\tau}\right)\cos(\varphi)\hat{e}_{y'} - \sin\left(\frac{\lambda_e \times r}{\tau}\right)\sin(\varphi)\hat{e}_{z'} \right) \quad 0 < r < \tau \tag{22}$$

$$\vec{V}_{X'Y'Z'} = |V| \times \frac{T(Q2 - Q1)}{|T(Q2 - Q1)|} \qquad r = 0 \tag{23}$$

Table 1 Variables for straight line path following

VARIABLE	DESCRIPTION
χ	Current ground track heading angle of the MAV
χ_f	Ground track heading angle along the path
χ_d	Ground track heading angle defined by the vector field
χ_c	Commanded ground track heading angle
γ	Current vertical flight path angle of the MAV
γ_f	Vertical flight path angle along the path
γ_d	Vertical flight path angle defined by the vector field
γ_c	Commanded vertical flight path angle
k	Transition gain
Q	Current position of the MAV
$Q1, Q1_x, Q1_y, Q1_z$	Waypoint 1 and its north, east and down components
$Q2, Q2_x, Q2_y, Q2_z$	Waypoint 2 and its north, east and down components
s^*	MAV progress along the path, $s^* \in [0,1]$
τ	Transition region boundary distance
r	The perpendicular distance of the MAV from the path
λ_e	The entry angle of the MAV (Figure 3a)
ϕ	The azimuth angle in cylindrical coordinate system(Figure 3a)
T	Transformation matrix from world coordinates to the new frame of reference (X', Y', Z') where the X' is along the path
u, v, w	The components of the vectors of the vector field in the new frame of reference
u1,v1,w1	The components of the vectors of the vector field in the world coordinate system

This vector field is converted into the world coordinate system X, Y, Z. Here r=0 is defined as a special case because the azimuth angle ϕ is not defined at r = 0.It may also be mentioned that the function "atan2" used for calculating the heading is discontinuous at χ = 180°. As a result of this the heading becomes multi-valued and unstable varying rapidly between ±180° (a branch cut). For this, it is important first to detect when the ground track heading angle will assume the value of 180°. This is defined to be the case when the X-coordinate of the next waypoint is less than the X-coordinate of the current waypoint while the Y-coordinate remains the same and the MAV lies in a certain radius of the specified path. For these conditions, the heading angle is fixed at 180° irrespective of its position to prevent the unstable behavior. The following Section gives the pseudo-code of the algorithm used.

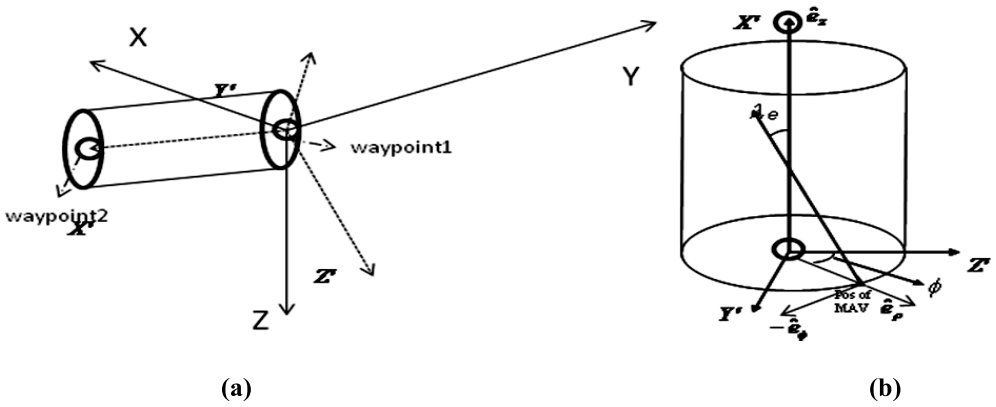

Figure 3. (a) Path coordinate system (X', Y', Z') and the world coordinate system (X, Y, Z) (b) Path coordinate system in cylindrical coordinates. $\hat{e}_z$, $\hat{e}_\rho$, $\hat{e}_\phi$ are unit vectors along the axis

4. PSEUDO CODE OF THE VECTOR FIELD CONSTRUCTION ALGORITHM

a) Calculate heading of the path:

$$\chi_f = \tan^{-1}\left(\frac{Q2_y - Q2_y}{Q1_x - Q1_x}\right)$$

b) Calculate vertical flight path angle along the path:

$$\gamma_f = \tan^{-1}\left(\frac{Q2_z - Q1_z}{\sqrt{\left(Q2_x - Q1_x\right)^2 + \left(Q2_y - Q1_y\right)^2}}\right)$$

c) Calculate transformation matrix

$$T = \begin{bmatrix} \cos(\gamma_f)\cos(\chi_f) & \cos(\gamma_f)\sin(\chi_f) & \sin(\gamma_f) \\ -\sin(\chi_f) & \cos(\chi_f) & 0 \\ -\sin(\gamma_f)\cos(\chi_f) & -\sin(\gamma_f)\sin(\chi_f) & \cos(\gamma_f) \end{bmatrix}$$

d) Transformation to X', Y', Z' axis
$Qnew = T \times (Q - Q_1)$

e) Calculate perpendicular distance from the path

$$r = \sqrt{Qnew_y^2 + Qnew_z^2}$$

f) Calculate the azimuth angle

$$\varphi = \tan^{-1}\left(\frac{Qnew_z}{Qnew_y}\right)$$

g) if $r < 1$
Switch to the next waypoint
Else
if $r > \tau$
Create the vector field outside the transition region

$u = \cos(\lambda_e)$
$v = -\sin(\lambda_e)\cos(\phi)$
$w = -\sin(\lambda_e)\sin(\phi)$
else if $r = o$
Create vector field on the path
$V = T(Q2 - Q1)$
$u = V_x$
$v = V_y$
$w = V_z$
else Create vector field in the transition region

$$u = \cos\left(\frac{\lambda_e r^k}{\tau^k}\right)$$

$$v = -\sin\left(\frac{\lambda_e r^k}{\tau^k}\right)\cos(\varphi)$$

$$w = -\sin\left(\frac{\lambda_e r^k}{\tau^k}\right)\sin(\varphi)$$

end if
h) Converting back to world coordinates

$$\begin{bmatrix} u1 \\ v1 \\ w1 \end{bmatrix} = T^{-1}\begin{bmatrix} u \\ v \\ w \end{bmatrix}$$

i) Calculate the vector field heading

$$\chi_d = \tan^{-1}\left(\frac{v1}{u1}\right)$$

j) Calculate γ specified by the vector field

$$\gamma_d = \tan^{-1}\left(\frac{w1}{\sqrt{v1^2 + u1^2}}\right)$$

k) if $r > \tau$
Calculate commanded heading and vertical flight path angle to autopilot for outside transition region
$\chi_c = \chi_d$
$\gamma_c = \gamma_d$
else
Calculate commanded heading and vertical flight path angle to autopilot for inside transition region

$$\chi_c = \chi_d - \left(\frac{k\lambda_e S}{\tau^k}\right) r^{k-1}\sin(\chi)$$

$$\gamma_c = \gamma_d - \left(\frac{k\lambda_e S}{\tau^k}\right) r^{k-1}\sin(\gamma)$$

end if
l) Condition to deal with discontinuity at π

if $(Q2_x < Q1_x) \,\&\, (Q2_y = Q1_y) \,\&\, (|r| < 4)$

$\chi_c = \pi$
end if
end if

To define the commanded ground track heading and the commanded vertical flight path angle the results of the stability analysis in [17, 19] are used. In [17, 19] the authors use Lyapunov stability arguments to show that the commanded ground track heading angle to direct the MAV to follow straight-line paths with asymptotically decaying error. This is assumed to apply to the vertical flight path angles as well.

With the commanded ground-track heading angle given above, algorithms which map the desired ground-track and altitude quantities into pitch and bank commands are used. This task is accomplished with a standard six degree of freedom autopilot system [18]. The numerical experiments and the simulations are described in the next section.

5. RESULTS AND DISCUSSION

The algorithm developed is tested for various simulated paths using a set of predefined waypoints in three dimensions as input. Simulation results showed effective, predictable, and safe navigation over a broad range of path types. Simulation results from an irregularly shaped path illustrating takeoff, descent and directional path following and control are shown in Figure 4. This situation is similar to the situation of the MAV navigating over a hill. The waypoints are shown as stars while the actual path is shown by the straight lines.

Fig. 4 (a) shows the results for the developed model after accounting for the discontinuity at $\chi = \pi$ and Fig. 5 shows the results for the developed model without accounting for the discontinuity at $\chi = \pi$. As expected, it is observed that the latter fails to follow the path after the fourth waypoint since $\chi_d = \pi$.

Figure 4. (a) Trajectory for path following after accounting for discontinuity at $\chi = \pi$ (b) Trajectory for path following without accounting for the discontinuity at $\chi = \pi$

The algorithm is then integrated with a 6 degree of freedom model for an MAV using the guidance, navigation and control system presented in [18]. The path following algorithm is used to provide the commanded ground track heading and vertical flight path angles to the PID controller. Figure 5 shows the same path as in figure 4 after integrating the path following algorithm with a 6 degree of freedom model of an aircraft. It was tested for four cases with different wind speeds. Fig 5(a) shows the case in which the wind speed was taken to be zero. Fig 5(b) shows the case in which the wind speed was given as 40% of the ground speed of the MAV. It was seen that in this case it missed the third waypoint by a margin of 1.1 m in travelling a distance of 800 m. Fig 5(c) shows the case in which the wind speed was given as 60% of the ground speed of the MAV. It was seen that in this case also it missed the third waypoint by a margin of 1.7 m in travelling a distance of 800 m. Fig 5(d) shows the case in which the wind speed was given as 80% of the ground speed of the MAV. It is observed that the MAV fails to follow the specified path after the third way point.

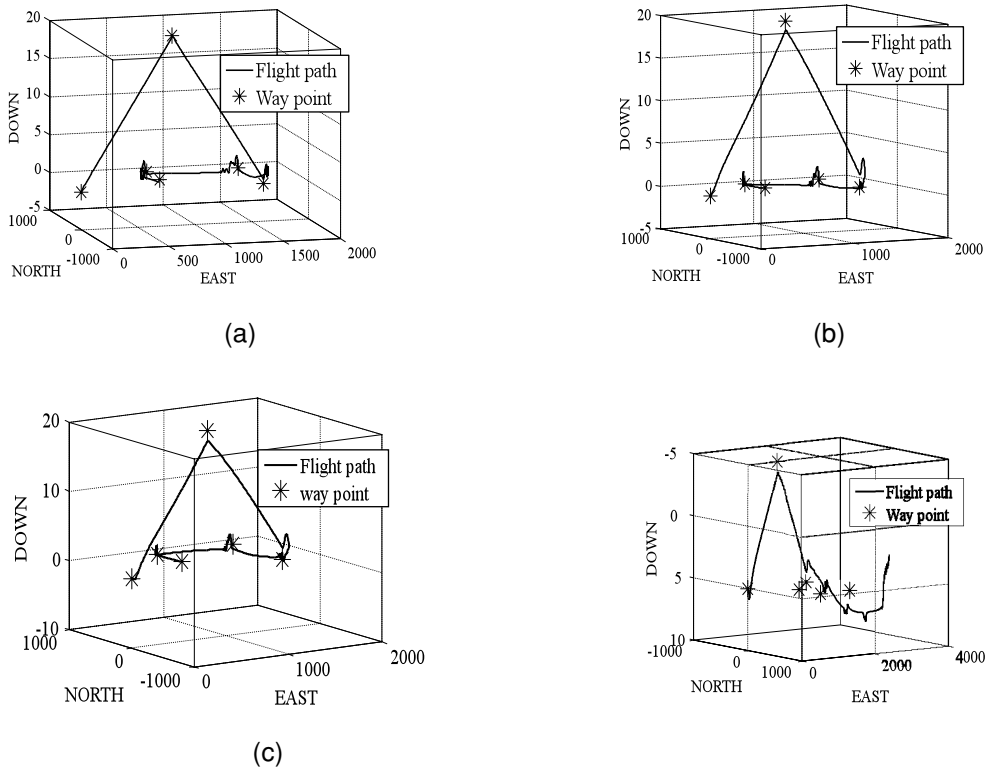

Figure 5. Trajectory with wind speed (a) zero (b) 40% of ground speed (c) 60% ground speed (d) 80% ground speed

Figure 6 shows the trajectory of a MAV with an initial error from the path and later converging onto the path, using the 6 degree of freedom model. It is observed that the trajectory of the MAV asymptotically converges to the specified path. It is observed that the MAV which starts at the origin gradually ascends and reaches the desired path and height. These types of maneuvers can be used for the takeoff or landing of the MAV.

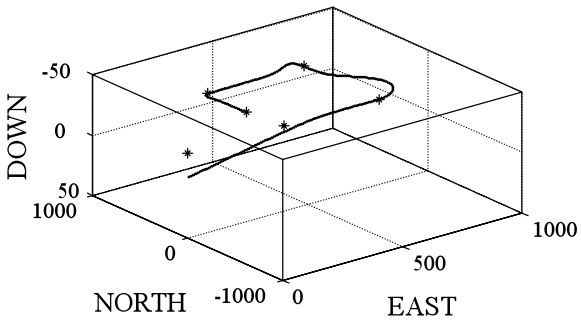

Figure 6. Trajectory of the MAV starting with an initial error

6. CONCLUSIONS

The idea of vector field path following in two dimensions has been extended to three dimensions by providing vertical flight path angle commands to the MAV. It has been shown using simulation that the tracking error has been reduced. Various scenarios were simulated, including the case where the MAV starts with an initial error and it is shown that the MAV gradually converges to the path.

The implementation of vector field path following is straight forward and the result is a robust algorithm for accurate path following. Controlling heading rate and pitch rate using ground track heading and vertical flight path angle, automatically accounts for the wind condition, thus reducing the error due to wind. By extending the algorithm to three dimensions we allow the aircraft to vary its altitude as well. As a result, the maneuverability of the aircraft is increased, allowing it to navigate in difficult terrain or engage in terrain following.

REFERENCES

[1] Nygard, K.E., Chandler, P.R., Pachter M., Dynamic network flow optimization models for air vehicle resource allocation, *Proc. of the American Control Conference*, June 2001, Arlington, Texas, 1853-1858.

[2] Schumacher, C., Chandler, P., Pachter, M., Pachter L.S., UAV task assignment with timing constraints, *AIAA Guidance, Navigation, and Control Conference and Exhibit*, August, Austin, Texas, 2003, AIAA 2003-5664.

[3] Schumacher, C., Chandler, P.R. , Rasmussen, S. J. , Walker D., Task allocation for wide area search munitions with variable path length, *Proc. of the American Control Conference*, June, Denver, Colorado, 2003, 3472-3477.

[4] Schumacher, C., Chandler, P.R. , Rasmussen, S. J., Task allocation for wide area search munitions via iterative network flow, *AIAA Guidance, Navigation, and Control Conference and Exhibit*, August, Monterey, California, 2002, AIAA 2002-4586.

[5] Chandler, P., Pachter, M, Rasmussen, S. J., Schumacher, C, Distributed control for multiple UAVs with strongly coupled tasks, *AIAA Guidance, Navigation, and Control Conference and Exhibit*, August, Austin, Texas, 2003, AIAA 2003-5799.

[6] Chandler, P., M. Pachter, M. , Rasmussen, S. J. , Schumacher C. Multiple task assignment for a UAV team, *AIAA Guidance, Navigation, and Control Conference and Exhibit*, August, Monterey, California, 2002, AIAA 2002-4587.

[7] Mitchell, J.W. , Chandler, P. , Pachter, M., Rasmussen S. J., Communication delays in the cooperative control of wide area search munitions via iterative network flow, *AIAA Guidance, Navigation, and Control Conference and Exhibit*, August, Austin, Texas, 2003, AIAA, 2003-5665.

[8] Curtis J.W. and Murphey R., Simultaneaous area search and task assignment for a team of cooperative agents, *AIAA Guidance, Navigation, and Control Conference and Exhibit*, August, Austin, Texas, 2003, AIAA 2003-5584.

[9] Turra, D. , Pollini, L. , Innocenti M.: Real-time unmanned vehicles task allocation with moving targets, *AIAA Guidance, Navigation, and Control Conference and Exhibit*, August, Providence, Rhode Island, 2004, AIAA 2004-5253.

[10] Blake Barber, D. , Joshua D. Redding, Timothy W. McLain, Randal W. Beard, Clark N. Taylor, Vision-based Target Geo-location using a Fixed-wing Miniature Air Vehicle *Journal of Intelligent and Robotic Systems*, 2006,vol. 47, no. 4, , 361-382.

[11] Kaminer, I., Pascoal, A. , Hallberg, E. and Silvestre, C. , Trajectory tracking for autonomous vehicles: An integrated approach to guidance and control *AIAA J. Guidance, Control Dynam.*, 1998, vol. 21, no. 1, pp. 29–38.

[12] P. Aguiar, J. Hespanha, and P. Kokotovic´, "Path-following for non-minimum phase systems removes performance limitations," *IEEE Trans. Automat. Control*, vol. 50, no. 2, pp. 234–239, Mar. 2005.

[13] Khatib, O., Real-Time Obstacle Avoidance for Manipulators and Mobile Robots, *The International Journal of Robotics Research,* March 1 1986,vol. 5, pp. 90-98,.

[14] Borenstein, J. and Koren, Y. Real-time obstacle avoidance for fast mobile robots," *IEEE Transactions on Systems, Man and Cybernetics*, 1989,vol. 19, pp. 1179-1187.

[15] Koren, Y. and Borenstein, J., Potential field methods and their inherent limitations for mobile robot navigation, *Proceedings of the IEEE International Conference on Robotics and Automation ICRA- 1991*, Sacramento, CA, April 1991 pp. 1398-1404.

[16] Koditschek, D., Exact robot navigation by means of potential functions: Some topological considerations, *Proceedings IEEE International Conference on Robotics and Automation ICRA-1987*, Raleigh, NC, 1987, pp. 1-6.

[17] Wei Ren, Randal W. Beard, Trajectory Tracking for Unmanned Air Vehicles with Velocity and Heading Rate Constraints," *IEEE Transactions on Control Systems Technology*, September, 2004,12, no. 5, p. 706-716.

[18] Gupta, V. V., Gandhi, P. S., Arya, H, Amitay Isaacs and Sudhakar, K. , Hardware-In-Loop Simulator for autonomous Navigation of Mini Aerial Vehicle, *2nd International Conference on Computational Intelligence, Robotics and Autonomous Systems (CIRAS 2003)*, 15-18 December, National University of Singapore, Singapore.

[19] Derek R. Nelson, Blake Barber, Timothy W. McLain, Randal W. Beard, "Vector Field Path Following for Miniature Air Vehicles," *IEEE Transactions on Robotics*, vol. 23, no. 3, June, 2007, 519-529.